

## Crystal structural phase transition in $\text{CaCrO}_4$ under high pressure

To cite this article: Y W Long *et al* 2006 *J. Phys.: Condens. Matter* **18** 2421

View the [article online](#) for updates and enhancements.

### You may also like

- [Magnetic states and magnetic transitions in  \$\text{RCo}\_2\$  Laves phases](#)  
X B Liu and Z Altounian
- [5th International Workshop on Top Quark Physics \(TOP2012\)](#)  
G Salamanna, V Boisvert, L Cerrito et al.
- [Forthcoming meetings](#)

# Crystal structural phase transition in $\text{CaCrO}_4$ under high pressure

Y W Long<sup>1</sup>, L X Yang<sup>1</sup>, S J You<sup>1</sup>, Y Yu<sup>1</sup>, R C Yu<sup>1</sup>, C Q Jin<sup>1,3</sup> and J Liu<sup>2</sup>

<sup>1</sup> Beijing National Lab for Condensed Matter Physics, Institute of Physics, Chinese Academy of Sciences, Beijing 100080, People's Republic of China

<sup>2</sup> Institute of High Energy Physics, Chinese Academy of Sciences, Beijing 100039, People's Republic of China

E-mail: [jin@aphy.iphy.ac.cn](mailto:jin@aphy.iphy.ac.cn)

Received 1 September 2005, in final form 6 January 2006

Published 10 February 2006

Online at [stacks.iop.org/JPhysCM/18/2421](http://stacks.iop.org/JPhysCM/18/2421)

## Abstract

Pressure-related structural properties of  $\text{CaCrO}_4$  with zircon-type structure ( $I4_1/amd$ ) at ambient pressure were investigated using synchrotron radiation x-ray diffraction in energy-dispersive mode in a diamond anvil cell (DAC) up to 29.1 GPa at room temperature. A sluggish first-order structural phase transition to a scheelite-type phase ( $I4_1/a$ ) was observed at 5.7 GPa. The lattice parameters of both phases at different pressures were calculated. The isothermal Birch–Murnaghan equation of state (EOS) was used to fit the data of pressure versus unit cell volume, and the bulk moduli were simulated to be  $103.7 \pm 0.3$  and  $125.1 \pm 6.2$  GPa for the zircon and scheelite phase, respectively.

## 1. Introduction

$\text{ABO}_4$ -type compounds with zircon or scheelite structure are technically important materials in the fields related to solid-state scintillator detectors [1, 2] optoelectronic devices [3, 4] and solid-state lasers [5, 6]. These materials also are attractive due to their interesting structural properties under high pressure. The crystal structure of zircon-type compounds with space group  $I4_1/amd$  (No. 141,  $Z = 4$ ) such as  $\text{RVO}_4$  ( $R = \text{Y, Tb, and Dy}$ ) [7–9] and  $\text{ASiO}_4$  ( $A = \text{Zr and Hf}$ ) [10–13] will transform into a scheelite phase in  $I4_1/a$  symmetry (No. 88,  $Z = 4$ ) under an appropriate pressure condition. Moreover, the scheelite structure is not very stable to pressure. Usually, at higher pressure, it will be replaced by either a monoclinic wolframite structure (space group:  $P2_1/c$ , No. 13,  $Z = 2$ ), or an M-fergusonite structure (space group:  $I2/a$ , No. 15,  $Z = 4$ ) or an M'-fergusonite structure (space group:  $P2_1/c$ , No. 14,  $Z = 2$ ) accompanying the decline of symmetry and the increase of coordination number of the B-site cation [14–23].

<sup>3</sup> Author to whom any correspondence should be addressed.

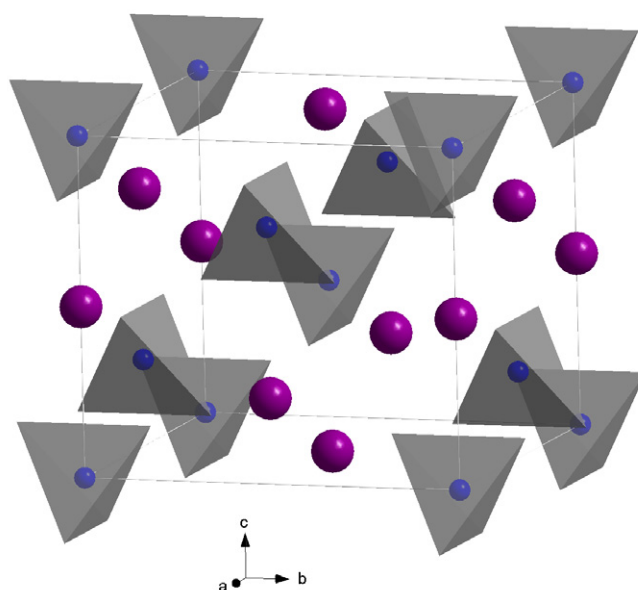


**Figure 1.** The crystal structure of the zircon-type  $\text{CaCrO}_4$  at ambient conditions. The larger and smaller balls represent the Ca and Cr atoms, respectively. The  $\text{CrO}_4$  tetrahedra are shown, but the O atoms at the vertex are omitted.

(This figure is in colour only in the electronic version)

$\text{CaCrO}_4$  crystallizes in a tetragonal zircon-type structure at ambient conditions. It is composed of chains of alternating edge-sharing  $\text{CrO}_4$  tetrahedra and  $\text{CaO}_8$  dodecahedra, as shown in figure 1. The  $\text{CrO}_4$  tetrahedra are somewhat elongated because the O–O edges shared with  $\text{CaO}_8$  dodecahedra are shorter than the length of the unshared tetrahedral edges [24]. Although the thermodynamic properties of  $\text{CaCrO}_4$  have been studied in detail [25–27], little is known about its high-pressure structural behaviour. Most recently, we have reported evidence of a pressure-induced structural phase transition in  $\text{CaCrO}_4$  based on high-pressure Raman scattering investigations [28]. We present here the high-pressure energy-dispersive x-ray diffraction (EDXRD) of  $\text{CaCrO}_4$ . The zircon-type  $\text{CaCrO}_4$  will evolve toward a scheelite phase upon increasing the pressure to 5.7 GPa. The pressure-related lattice parameters, unit cell volumes as well as the equations of state for the zircon- and scheelite-type  $\text{CaCrO}_4$  are reported.

## 2. Experimental methods

The highly pure  $\text{CaCrO}_4$  polycrystalline powder used in this experiment was prepared by standard solid-state reaction methods [24]. The *in situ* high-pressure EDXRD experiments were carried out at the Beijing Synchrotron Radiation Facility (BSRF) using a DAC with 500  $\mu\text{m}$  culet in the pressure range from 1.6 to 29.1 GPa at room temperature. T301 stainless steel was used as a gasket in which a 250  $\mu\text{m}$  hole was drilled to serve as the sample chamber. In order to generate a hydrostatic pressure condition, a 4:1 methanol–ethanol mixture was used as the pressure medium. Pressures were calibrated using the ruby luminescence method [29]. The optimum diffraction angle  $2\theta$  was set to  $15.4^\circ$  to obtain sufficient and discernable diffraction peaks.

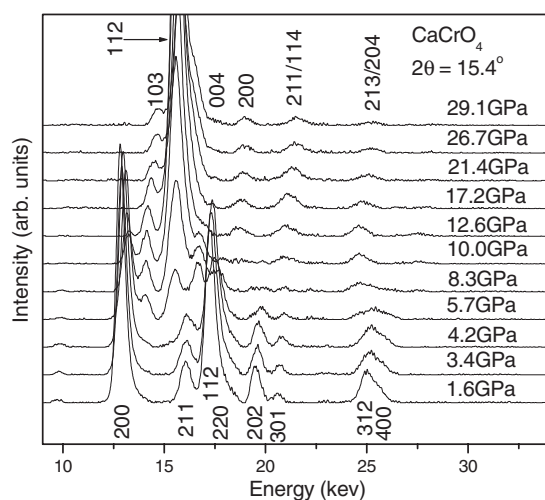
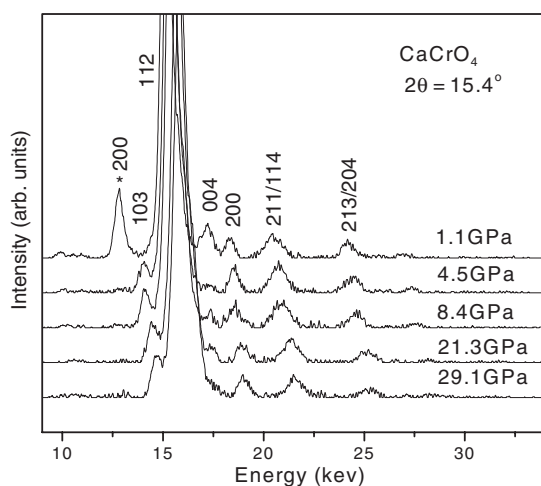


**Figure 2.** Some typical EDXRD patterns of CaCrO<sub>4</sub> during the compression process from 1.6 to 29.1 GPa. A structural phase transition is indicated at 5.7 GPa.

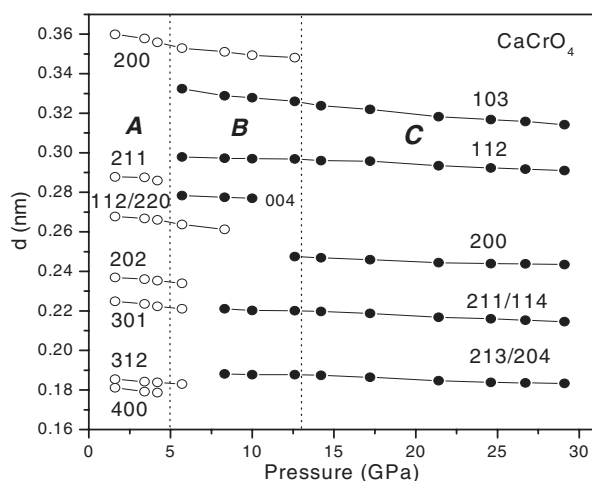
### 3. Results and discussion

Figure 2 shows some typical EDXRD patterns collected in the compression process from 1.6 to 29.1 GPa. Seven diffraction peaks of the zircon-type CaCrO<sub>4</sub> (the (112) and (220) peaks are overlapped) are observed at the starting pressure 1.6 GPa. Diffraction diagrams show that the zircon phase of CaCrO<sub>4</sub> can be stably preserved up to 4.2 GPa. In this pressure range, all the diffraction peaks slowly shift towards the higher-energy direction with increasing pressure. However, when the pressure increases to 5.7 GPa, three new diffraction peaks clearly appear at 13.92, 15.57 and 16.62 keV, respectively, concomitant with the disappearance of the (211) peak and the sharp decline in diffraction intensity of the zircon phase. These are indicative of a pressure-driven structural phase transition from zircon to scheelite in CaCrO<sub>4</sub> at 5.7 GPa. However, the zircon phase will coexist with the new scheelite phase until 12.6 GPa. Between 12.6 and 29.1 GPa, only the scheelite-phase diffraction peaks are observed as shown in figure 2. In addition, it is notable that the diffraction peaks gradually become broader with pressure, which implies an increasing pressure gradient in the sample.

In succession, when the pressure is gradually released from 29.1 to 4.5 GPa, none but the scheelite-phase diffraction peaks are discernible as shown from the decompressed EDXRD diagrams in figure 3. However, as the pressure decreases to the lowest, about 1.1 GPa, the (103) peak of the scheelite phase becomes indiscernible (perhaps it overlaps with the (112) peak that scheelite compounds usually exhibit at ambient conditions). In addition, the strongest (200) peak of the zircon-type CaCrO<sub>4</sub> reemerges, which most probably results from the deviation of diffraction spot from the central region of the sample chamber due to an accidental slight movement of the gasket in decompression. On account of the pressure gradient existing in the sample, the structural transition is probably not completed thoroughly in the edge part of the sample chamber. In our high-pressure Raman scattering experiment on CaCrO<sub>4</sub> [28], no zircon-phase Raman active mode was observed when the pressure was released from 26.2 to 0.1 GPa. Therefore, we believe that the structural phase transition from zircon to scheelite in CaCrO<sub>4</sub> observed here at 5.7 GPa is nonreversible, just like other isostructural compounds have exhibited [7–13].



**Figure 3.** EDXRD diagrams of  $\text{CaCrO}_4$  during the decompression progress. The star denotes the (200) peak of the zircon phase.



**Figure 4.** Pressure dependence of  $d$ -values of  $\text{CaCrO}_4$  during the compression process. Open and solid circles correspond to the zircon and scheelite phase, respectively. The three regions *A*, *B*, and *C* show different structural properties.

Based on the scheelite-phase model, all the diffraction peaks of the new phase can well be indexed, as shown in figures 2 and 3. The  $d$ -values corresponding to the diffraction peaks of both phases at different pressures were calculated according to the formula  $E = 6.199/d \sin(\theta)$ , where  $E$  is the energy of each diffraction peak, and  $\theta$  equals  $7.7^\circ$  in this experiment. From figure 4 it is obvious that the  $d$ -values of both phases gradually decrease with pressure in the whole compression process. In addition, three pressure regions related to different structural characteristics are displayed. The zircon-type phase only can be stably retained in region *A*, the pressure range from 0 to 5 GPa. In region *B*, from 5 to 13 GPa, the scheelite phase starts to appear and coexists with the zircon phase. This structural transition is somewhat sluggish under high pressure, and a moderate pressure range is needed to complete

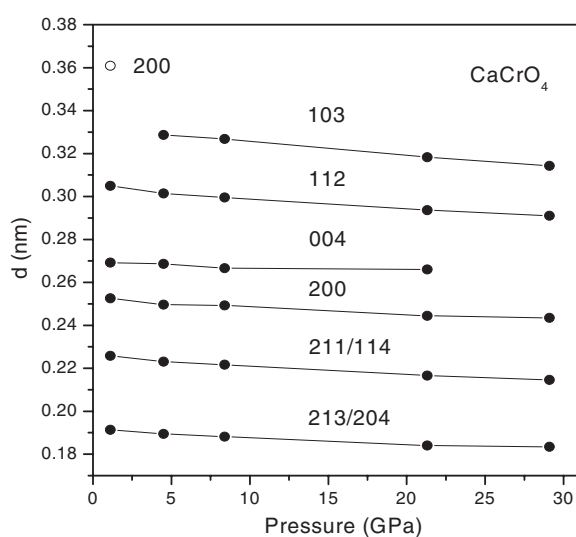


**Figure 5.** Pressure dependence of  $d$ -values of CaCrO<sub>4</sub> during the decompression progress. Open and solid circles correspond to the zircon and scheelite phase, respectively.

the transition. This perhaps is a common characteristic for the structural transition of zircon-type compounds under hydrostatic pressure conditions [9, 11, 12, 28]. The zircon phase is fully replaced by the scheelite phase in region *C* when the pressure exceeds 13 GPa. Moreover, no post-scheelite phase appears up to the highest pressure 29.1 GPa we used.

Correspondingly, the pressure dependence of  $d$ -values in the decompression process is shown in figure 5. When the pressure is decreased to 4.5 GPa, only the scheelite phase is observed. In addition, the (004) peak of the scheelite phase returns at 21.3 GPa. Although the zircon-phase (200) peak is observed at 1.1 GPa, we regard the structural transition as a nonreversible one, as mentioned above.

Based on the  $d$ -values and the relevant indices, the lattice parameters and unit cell volumes as a function of pressure were obtained as presented in figures 6 and 7, respectively. For the zircon-type CaCrO<sub>4</sub>, the longer  $a$ -axis is more compressible than the shorter  $c$ -axis, and the axial ratio  $c/a$  gradually increased with pressure as the inset shows in figure 6, which indicates an anisotropic compressibility in the zircon phase. This is not difficult to understand from the construction of the zircon-type CaCrO<sub>4</sub> that the larger CaO<sub>8</sub> dodecahedra directly align along the  $a$ -axis while the compacted CrO<sub>4</sub> tetrahedra alternately arrange with CaO<sub>8</sub> dodecahedra in the  $c$ -axis direction, just like figure 1 shows. As far as the scheelite phase is concerned, the data of the lattice parameters come from the compression process at pressure above 10 GPa. Below this pressure, the data come from the decompression process. Therefore, an anomalous increase of the longer  $c$ -axis with pressure is observed around 10 GPa due to the hysteretic effect of the first-order phase transition. Generally speaking,  $c/a$  will gradually increase with pressure for zircon-type ABO<sub>4</sub> compounds, while the reverse is true for scheelite-type ABO<sub>4</sub> compounds [9].

Using the isothermal Birch–Murnaghan equation of state (EOS) with the format  $P(\text{GPa}) = \frac{3}{2}B_0\left[\left(\frac{V_0}{V}\right)^{\frac{2}{3}} - \left(\frac{V_0}{V}\right)^{\frac{5}{3}}\right]\left\{1 - \left(3 - \frac{3}{4}B'_0\right)\left[\left(\frac{V_0}{V}\right)^{\frac{2}{3}} - 1\right]\right\}$  ( $V$  and  $V_0$  represent the high-pressure and ambient-pressure unit cell volume, respectively;  $B_0$  and  $B'_0$  refer to the bulk modulus and its pressure derivative), the relationship of pressure versus unit cell volume was fitted as shown in figure 7. The bulk modulus  $B_0$  of the zircon-type CaCrO<sub>4</sub> is well simulated to be

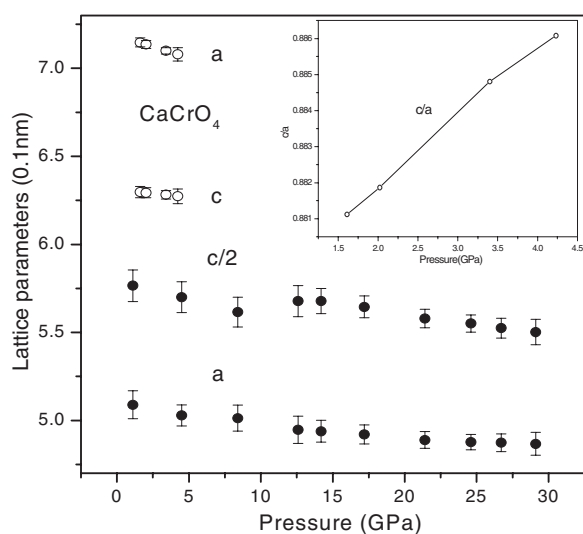


**Figure 6.** Lattice parameters as a function of pressure in CaCrO<sub>4</sub>. Open and solid circles correspond to the zircon and scheelite phase, respectively. The inset shows the pressure dependence of the axial ratio *c/a* for the zircon-type CaCrO<sub>4</sub> in the range 1.6–4.2 GPa.

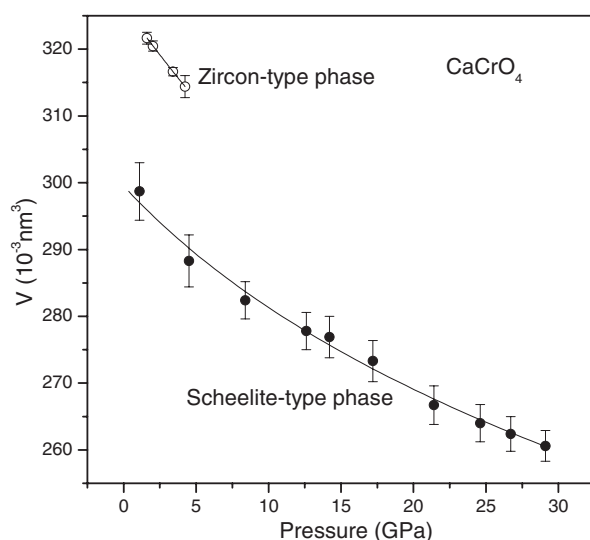


**Figure 7.** Unit cell volume as a function of pressure in CaCrO<sub>4</sub>. Open and solid circles correspond to the zircon and scheelite phase, respectively. The solid curves are the fitting results from the isothermal Birch–Murnaghan EOS.

$103.7 \pm 0.3$  GPa assuming its pressure derivative  $B'_0 = 4$ , and  $V_0$  was extrapolated to be  $326.52 \pm 0.02 \text{ \AA}^3$ , a similar value to the single-crystal experimental result ( $327.81 \text{ \AA}^3$ ) [24].

Recently, Errandonea *et al* have proposed an experiential criterion,  $B_0$  (GPa) =  $(610 \pm 110)Z_A/d_{A-O}^3$ , to evaluate the bulk modulus for zircon- and scheelite-type ABX<sub>4</sub> compounds [22], where  $Z_A$  is the formal charge for the A cation, and  $d_{A-O}$  is the average A–O distance (in  $\text{\AA}$ ) inside the AO<sub>8</sub> polyhedron at ambient conditions. In terms of the average

Ca–O bond length 2.37 Å, the bulk modulus of the zircon-type CaCrO<sub>4</sub> was calculated to be  $92 \pm 15$  GPa, which is in good accordance with our experimental result.

As to the scheelite phase of CaCrO<sub>4</sub>,  $B_0$  and  $B'_0$  were simulated to be  $125.1 \pm 6.2$  GPa and  $7.3 \pm 1.2$ , respectively. In the same way,  $V_0$  was obtained to be  $299.5 \pm 2.0$  Å<sup>3</sup>. In the light of the simulated results, it is known that the bulk modulus increases by about 20%, and the ambient-pressure unit cell volume decreases by about 9% in the structural transition from zircon to scheelite in CaCrO<sub>4</sub>. These changes can be ascribed to a more efficient arrangement of the coordination polyhedra and the elimination of some structural holes in the zircon-type structure [30]. Consequently, the scheelite phase is more difficult to be compressed than the zircon phase. In addition, the jump of  $V_0$  in both phases indicates that this structural phase transition is a first-order transition.

Kusaba *et al* [10] reported a fast structural phase transition (less than 1 μs) of the zircon-type ZrSiO<sub>4</sub> to a scheelite phase under shock compression, and put forward a mechanism for this structural transition. In terms of their expression, the density would increase by about 10% when a zircon phase transformed into a scheelite phase. In our experiment, a 9% reduction of  $V_0$  is consistent with their results.

#### 4. Conclusion

To sum up, high-pressure EDXRD was performed on CaCrO<sub>4</sub> at room temperature in the 0–29.1 GPa pressure range. A nonreversible crystal structural phase transition from zircon to scheelite was observed at 5.7 GPa. The pressure dependence of  $d$ -values exhibits a series of pressure-related structural properties. The zircon phase of CaCrO<sub>4</sub> is stable about below 5 GPa, and the scheelite phase coexists with the zircon phase until the pressure exceeds 13 GPa. The axial ratios ( $c/a$ ) at different pressures reveal an anisotropic compressibility for the zircon-type CaCrO<sub>4</sub>. The relationship between pressure and unit cell volume was fitted using the isothermal Birch–Murnaghan EOS, and the bulk moduli were simulated to be  $103.7 \pm 0.3$  and  $125.1 \pm 6.2$  GPa for the zircon and scheelite CaCrO<sub>4</sub>, respectively. The increases of bulk modulus and density in the phase transition imply the more efficient packing of coordination polyhedra in the scheelite phase.

#### References

- [1] Ishii M and Kobayashi M 1991 *Prog. Cryst. Growth Charact.* **23** 245
- [2] Chernov S, Deych R, Grigorjeva L and Millers D 1997 *Mater. Sci. Forum* **239** 299
- [3] Nikl M, Bohacek P, Mihokova N, Solovieva N, Vedda A, Martini M, Pazzi G P, Fabeni P, Kobayashi M and Ishii M 2002 *J. Appl. Phys.* **91** 5041
- [4] Brenier A *et al* 2004 *J. Phys.: Condens. Matter* **16** 9103
- [5] Blasse G 1966 *J. Chem. Phys.* **45** 2356
- [6] Brecher C, Samelson H, Lempicki A, Riley R and Peters T 1967 *Phys. Rev.* **155** 178
- [7] Jayaraman A, Kourouklis G A, Espinosa G P, Cooper A S and Van Uitert L G 1987 *J. Phys. Chem. Solids* **48** 755
- [8] Duclos S J, Jayaraman A, Kourouklis G A, Cooper A S and Maines R G 1989 *J. Phys. Chem. Solids* **50** 769
- [9] Wang X, Loa I, Syassen K, Hanfland M and Ferrand B 2004 *Phys. Rev. B* **70** 064109
- [10] Kusaba K, Yagi T, Kikuchi M and Syono Y 1986 *J. Phys. Chem. Solids* **47** 675
- [11] Knittle E and Williams Q 1993 *Am. Mineral.* **78** 245
- [12] Van Westrenen W, Frank M R, Hanchar J M, Fei Y, Finch R J and Zha C S 2004 *Am. Mineral.* **89** 197
- [13] Liu L 1986 *Earth Planet. Sci. Lett.* **57** 110
- [14] Nicol M and Durana J F 1971 *J. Chem. Phys.* **54** 1436
- [15] Shieh S R, Ming L C and Jayaraman A 1996 *J. Phys. Chem. Solids* **57** 205
- [16] Sen A, Chaplot S L and Mittal R 2002 *J. Phys.: Condens. Matter* **14** 975  
Sen A, Chaplot S L and Mittal R 2003 *Phys. Rev. B* **68** 134105



- [17] Grzechnik A, Crichton W A, Hanfland M and Van Smaalen S 2003 *J. Phys.: Condens. Matter* **15** 7261
- [18] Li S, Ahuja R, Wang Y and Johansson B 2003 *High Pressure Res.* **23** 343
- [19] Panchal V, Garg N, Chauhan A K, Sangeeta B and Sharma S M 2004 *Solid State Commun.* **130** 203
- [20] Li S, Ahuja R and Johansson B 2004 *J. Phys.: Condens. Matter* **16** S983
- [21] Errandonea D, Manjón F J, Somayazulu M and Häusermann D 2004 *J. Solid State Chem.* **177** 1087
- [22] Errandonea D, Porres J P, Manjón F J, Segura A, Roca C F, Kumar R S, Tschauner O, Hernández P R, Solano J L, Radescu S, Mújica A, Muñoz A and Aquilanti G 2005 *Phys. Rev. B* **72** 174106
- [23] Panchal V, Garg N and Sharma S M 2005 *Preprint* [cond-mat/0505443](#)
- [24] Weber G and Range K J 1996 *Z. Naturf. b* **51** 751
- [25] Clark R P, Gallagher P K and Dillard B M 1979 *Thermochim. Acta* **33** 141
- [26] Wang T G and Li Z H 2004 *J. Chem. Eng. Data* **49** 1300
- [27] Lee Y M and Nassaralla C L 2001 *Thermochim. Acta* **371** 1
- [28] Long Y W, Zhang W W, Yang L X, Yu Y, Yu R C, Ding S, Liu Y L and Jin C Q 2005 *Appl. Phys. Lett.* **87** 181901
- [29] Mao H K, Xu J and Bell P M 1986 *J. Geophys. Res.* **91** 4673
- [30] Reid A F and Ringwood A E 1969 *Earth Planet. Sci. Lett.* **6** 205